

# The composition of insoluble intermetallic phases in aluminium alloy 6010

P. HODGSON\*, B. A. PARKER

*Department of Materials Engineering, Monash University, Clayton, Victoria 3168, Australia*

Insoluble intermetallic particles have been extracted from the complex Al (Mg, Si, Cu, Mn, Cr, Fe) alloy (designated 6010) using an extraction solution containing 8-hydroxyquinoline. The extracted particles were analysed using both X-ray diffraction and energy dispersive analysis techniques in the transmission electron microscope. The particles were found to be the cubic  $\alpha$ -Al(Fe Mn)Si phase. Analysis showed two distinct compositions for the phase: larger particles ( $> 0.5 \mu\text{m}$ ) had a much higher iron content and lower silicon content than smaller particles. The absorption of other solute elements into these particles during an ageing treatment was noted.

## 1. Introduction

Commercial, age-hardened aluminium alloys contain a number of second-phase particles, some of which are present because of deliberate alloying additions and others of which arise from common impurity elements and their interactions. This paper is concerned with the intermetallic particles which form either on solidification or whilst the alloy is at a relatively high temperature in the solid state, for example, during homogenization, solution treatment or recrystallization. The size, shape and distribution of these particles may have important effects on the ductility of alloys and more needs to be known regarding their formation, structure and composition.

To date, the nature of many intermetallic and impurity phases has been established using metallographic techniques, X-ray diffraction and electron-probe microanalysis. Most of this information has been obtained from particles grown by special treatments to a size where they are amenable to the investigative technique. The results obtained are not always representative of phases present following commercial heat-treatment.

In steels and some non-ferrous alloys phase identification has been achieved by particle extraction either in bulk for X-ray diffraction, see for example [1], or in the form of extraction replicas

for electron microscopy and electron diffraction, see for example [2]. In aluminium alloys particle extraction is difficult as, under the majority of conditions, the second phases appear to dissolve more readily than the matrix.

Recently, success has been reported in the use of a complexing agent to change the solubility of aluminium relative to the particles. The use of oxine (8-hydroxyquinoline) was reported initially by Honda and Hirokawa [3] and an improved method was described by Cocks, Shephard and Chilton [4]. The technique was subsequently applied to the extraction of phases in alloys 2036, 6061 and 7075 [5]. X-ray diffraction was used to identify the extracted particles. Some success has been reported with the agent nitrolotri-acetic acid in extracting particles from Al-Zn-Mg-Cu alloys [6].

In the work reported here we have used the oxine reagent to extract particles from alloy 6010 introducing some modifications to the methods described earlier. The extracted particles have been examined both by X-ray diffraction and energy dispersive X-ray analysis in the transmission electron microscope. The advantage of this study is that information on composition as well as crystallography has been obtained and changes in particle composition during heat-treatment have been followed.

\*Present address: B.H.P. Melbourne Research Laboratories, Clayton, Victoria 3168, Australia.

## 2. Experimental procedure

### 2.1. Alloy and heat treatment

A sample of the commercial aluminium alloy 6010 in the T4 condition was the starting material. The composition of alloy 6010 is approximately 0.33 wt% Cu, 0.8 wt% Mg, 0.33 wt% Mn, 1.0 wt% Si, 0.5 wt% Fe, 0.02 wt% Ti, balance aluminium. The effect on particle composition of an additional ageing treatment simulates that which might be expected in a paint bake cycle following the forming of a part from the material.

### 2.2. Particle extraction

#### 2.2.1. Chemical extraction

0.3 g of alloy 6010 was dissolved in a solution similar to that used by Honda and Hirokawa [3]: 15 g 8-hydroxyquinoline, 60 g benzoic acid, 60 ml chloroform, 150 ml methanol and 0.02 g NaOH. The solution was magnetically stirred. Reaction proceeded slowly, there being no noticeable dissolution after seven days, complete dissolution taking ten days. The solution was carefully decanted leaving 50 ml containing the particles, this suspension was centrifuged at 1000 g for ten min. The residue was washed alternately with methanol and chloroform to ensure that no organic contamination remained.

#### 2.2.2. Electrochemical extraction

Chemical attack of aluminium is inhibited by the oxide film on the surface. Cocks *et al.* [4] suggested that the role of the sodium hydroxide in the chemical extraction solutions was to promote attack of the oxide layer, the low concentration making this a slow process and they suggested, as an alternative, the electrochemical removal of the oxide layer.

A modified form of the solutions was used in order to facilitate subsequent cleaning and to reduce the level of precipitation in the solution. The most satisfactory composition was 15 g 8-hydroxyquinoline, 60 g benzoic acid, 80 ml chloroform and 200 ml methanol. An applied current of 10 mA was used. It was noted, following a suggestion by Cocks *et al.*, that the function of the applied current was solely to break up the oxide film and that it had little effect on the rate of dissolution. In view of the relatively long dissolution times and the flammability of the constituents in the solution, the current was applied only for the first 20 min and the reaction then proceeded unaided.

1 g of alloy 6010 was dissolved in 10 h and the residue was centrifuged and cleaned as described above. The amount dissolved is some three times greater than that obtained with an equivalent amount of 8-hydroxyquinoline by Cocks *et al.* and it is probable that the additional solvent facilitates extraction by preventing the precipitation of the aluminium complex. It was necessary to centrifuge the solution within 12 h of dissolution or precipitation occurred; the precipitate that forms is insoluble in the solvents present.

### 2.3. X-ray diffraction

Extracted particles were ultrasonically dispersed in methanol and the suspension allowed to dry on a glass slide. This enabled satisfactory X-ray diffraction traces to be obtained using the small quantity of material available with the minor disadvantage that the amorphous scattering peaks from the glass had to be subtracted before determining relative peak intensities. Nickel-filtered copper radiation was used.

### 2.4. Electron microscopy and microanalysis

Samples, dispersed in methanol, were allowed to dry on carbon films supported on graphite grids. Particles were examined using a JEOL 100C transmission electron microscope equipped with scanning and energy dispersive microanalysis facilities. The microscope had been modified, to reduce the background X-ray count, by using an auxiliary aperture above the sample and by using graphite specimen holder components.

An advantage of the analysis of extracted particles on a supporting carbon film is that there is no matrix to scatter the beam, reducing the amount of stray X-ray radiation scattered from the vicinity of the objective lens pole-piece. A large number of particles was studied and information gained on the morphology, size and emitted X-ray spectra. X-ray spectra were converted to details of the chemical composition using the *K*-factors given by Lorimer and Cliff [7] for standard-less thin-film analysis.

## 3. Results

### 3.1. Particle size and morphology

Some examples of the extracted particles are shown in Fig. 1. In both as-received (T4) and artificially-aged conditions two distinct groups of particles were found:

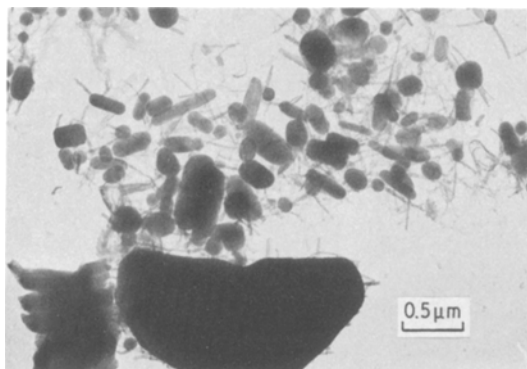


Figure 1 Particles seen in the TEM following extraction by 8-hydroxyquinoline.

(a) large ( $> 0.5 \mu\text{m}$ ) irregular particles ranging in size up to  $20 \mu\text{m}$ ;

(b) particles less than  $0.5 \mu\text{m}$  having a spherical, spheroidal or cylindrical shape. These particles had a minimum dimension of around  $0.2 \mu\text{m}$  and aspect ratios ranged from 1:1 to 6:1. No evidence was found for the fine  $\text{Mg}_2\text{Si}$  age-hardening phase and it is unlikely that it was extracted.

### 3.2. X-ray diffraction

A characteristic of the X-ray traces was the presence of pairs of peaks suggesting two phases of similar structure but slightly different lattice parameter. The peaks with the lower  $d$ -spacing had the higher intensity indicating its presence in greater quantity. The phases were indexed as cubic with lattice parameters of 1.258 and 1.260 nm (a measurement error of  $\pm 2 \times 10^{-3}$  nm was determined for the absolute values). Accurate intensity data were not obtained for the weaker lines; the stronger lines gave intensities and  $d$ -spacing values similar to the phase ascribed the formula  $\text{Mn}_{12}\text{Si}_7\text{Al}_5$  by Cogan *et al.* [5], presumably from data in the ASTM powder diffraction file [8]. There are, however, differences in the intensities of some major lines compared with those reported in the file and those reported by Cogan *et al.* and measured in the present work. The phase appears to be body-centred cubic but it may be simple cubic with weak lines for odd values of  $h^2 + k^2 + l^2$  [9]. This phase, also known as the  $\alpha$ -aluminium–manganese silicide has been attributed a number of formulae and Mondolfo [10] gives  $(\text{Fe Mn})_3\text{Si}_2\text{Al}_{15}$  whereas Warlimont [11] quotes  $(\text{Fe Mn})_3\text{SiAl}_{12}$ . We shall comment further on the composition of the phase in a later section. Mondolfo notes that most of the manganese in  $\text{Mn}_3\text{Si}_2\text{Al}_{15}$

can be replaced by iron to a maximum level of 31 wt% iron, 1.5 wt% manganese and he notes further that iron addition causes a reduction in the lattice parameter from 1.265 to 1.25 nm at 31 wt% iron concentration. Mondolfo also states that chromium replaces iron and manganese in the  $\alpha$ -phase and that copper mainly replaces silicon. The results from the present work suggest that two forms of  $\alpha$ -phase are present, an iron-rich form with a lattice parameter 1.258 nm and one with lower iron content of lattice parameter 1.260 nm.

### 3.3. Particle composition

#### 3.3.1. As-received samples (solution treated and naturally aged)

Analysis, using the TEM of approximately 200 extracted particles showed distinct differences in composition between the large ( $> 0.5 \mu\text{m}$ ) and small particles. This difference was most obvious in the Mn/Fe ratio. The average compositions are presented in Table IA and B, divided into these two size classes. Data are presented both for the as-received (T4) samples and for samples aged at  $200^\circ\text{C}$ .

In addition to the elements reported in Table I, magnesium was found in some aged samples and titanium, up to a content of  $\sim 1$  wt%, was found in many particles. Approximately 2% of the particles analysed were not  $\alpha$ -phase, some of those analysed were of form close to  $\text{Al}_6(\text{Fe Mn})$  and a few appeared to contain only Fe, Mn or Cr and Cu with less than 5 wt% Al. The analyses in Table I were obtained from raw intensity data using the ratio method and the experimental  $K$ -factors of Lorimer and Cliff [7].

The application of the thin-film approximation can only be made if absorption of the emitted X-rays can be ignored. Goldstein [12] has recently reviewed criteria to be satisfied to meet this condition and applying these to the present work shows that the error introduced by not making absorption corrections is less than 2 wt% in the silicon content (silicon is the worst affected element) for  $0.1 \mu\text{m}$  particles rising to about 10% for  $0.5 \mu\text{m}$  particles. The majority of particles in the  $< 0.5 \mu\text{m}$  group were between 0.1 and  $0.2 \mu\text{m}$  in thickness in the direction of the electron beam. For the group of particles of size over  $0.5 \mu\text{m}$ , where typical dimensions of analysed particles were of the order of 1 to  $2 \mu\text{m}$ , the absorption of silicon and, to some extent, aluminium becomes significant. For  $1 \mu\text{m}$  particles the absorption

TABLE IA Compositions of extracted particles of size less than 0.5  $\mu\text{m}$ 

Sample treatment	Al (wt%)	Si (wt%)	Mn (wt%)	Fe (wt%)	Cu (wt%)	Cr (wt%)	Mn/Fe ratio
As-received	58.2	9.5	23.2	3.9	1.6	3.6	5.9
0.5 h at 200° C	57.5	7.6	24.6	5.1	2.2	3.1	4.9
24 h at 200° C	52.6	15.3	19.5	4.0	5.8	2.8	5.0
360 h at 200° C	50.6	15.9	20.2	5.1	5.5	2.7	4.1

TABLE IB Composition of extracted particles of size greater than 0.5  $\mu\text{m}$ 

Sample treatment	Al (wt%)	Si (wt%)	Mn (wt%)	Fe (wt%)	Cu (wt%)	Cr (wt%)	Mn/Fe ratio
As-received	58.2	3.2	13.0	22.0	2.4	0.8	0.59
0.5 h at 200° C	55.9	3.3	15.6	22.8	1.8	0.6	0.68
24 h at 200° C	60.1	4.4	12.8	20.1	1.7	0.9	0.64
360 h at 200° C	56.3	4.0	13.4	23.6	1.6	1.1	0.57

factor for silicon is 1.25 rising to 1.75 at 2  $\mu\text{m}$ ; equivalent factors for aluminium are 1.09 and 1.43, respectively. The absorption of *K* X-ray lines for the other elements is much less and can be neglected. The absorption correction cannot be accurately applied because the X-ray path length in these irregularly shaped particles is not known, however, it would seem reasonable to increase the relative amount of silicon by 50% and that of aluminium by 20% for these particles. The normalized composition then becomes approximately:

$$\begin{aligned} & \text{Al } 62 \text{ wt\%, Si } 4.6 \text{ wt\%, Mn } 11.5 \text{ wt\%,} \\ & \text{Fe } 19.4 \text{ wt\%, Cu } 2.1 \text{ wt\%, Cr } 0.7 \text{ wt\%} \quad (1) \end{aligned}$$

The (Mn + Fe) level of approximately 30% is reasonable for the  $\alpha$ -phase [9], however, the level of silicon remains very low suggesting that aluminium atoms are able to occupy silicon sites in the  $\alpha$ -structure. The larger particles contain significantly less chromium than the smaller ones.

The particle analyses confirm the X-ray diffraction results which suggested the presence of two variants of the  $\alpha$ -phase. The large particles are iron-rich and form the greatest volume fraction of the extracted phases.

### 3.3.2. The effect of ageing on the composition of the $\alpha$ -phase

Table I includes data on the effect of ageing on the composition of the  $\alpha$ -phase. It can be seen that there is little significant change in the composition of the large particles except for small decreases in copper content and increases in the chromium content. The variations in aluminium and silicon levels could be due to particle size effects on absorption.

The data for the small particles are re-plotted in Fig. 2 as a function of ageing time at 200° C. It can be seen that the silicon and copper content levels rise and that the (Fe + Mn) and aluminium content levels fall. There is also a fall in the (Mn/Fe) ratio. The chromium level remains nearly constant.

The (Si + Cu) content level, greater than 20 wt%, is higher than expected for the  $\alpha$ -phase. It was noted earlier that copper can replace silicon in the  $\alpha$ -structure and it was suggested in the previous section that silicon may be interchangeable with aluminium. An alternative explanation for the increased (Si + Cu) content levels may be that Si and Cu are absorbed onto the particles during ageing and do not enter the  $\alpha$ -structure. Changes of composition near the periphery of particles in an Al-Mn alloy were reported by Morris and Duggan [13]. The removal of copper and silicon by the  $\alpha$ -phase reduces their effectiveness as age-hardening elements, however, no measure of the total amount removed was obtained in this work.

The change in Mn/Fe ratio during ageing is probably due to variations in the Mn:Fe ratios in individual particles: these elements are almost completely interchangeable and wide variations were noted.

## 4. General discussion

The aluminium-manganese-iron-silicide phase is important in many aluminium alloys since it occurs in most commercial age hardening alloys. When it forms on solidification it is frequently the largest particle present and can give rise to poor ductility. The precipitation of the phase during high temperature heat treatment (homogen-

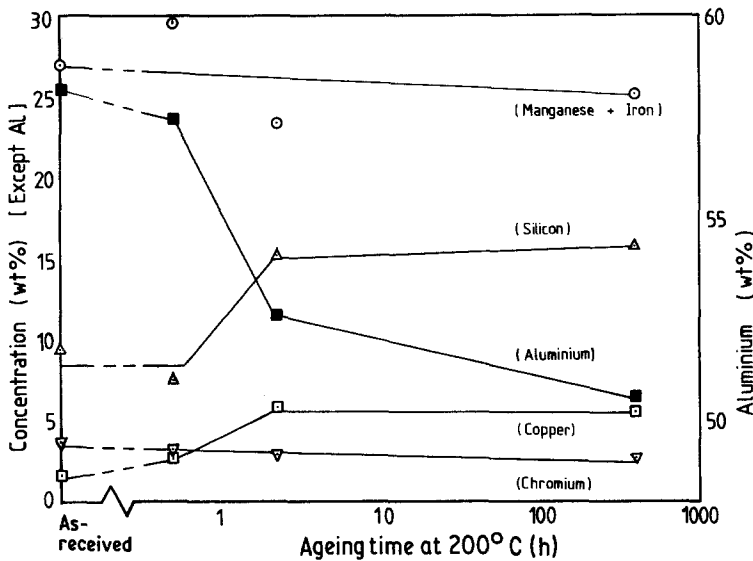


Figure 2 Variations in particle composition following ageing treatments at 200° C.

ization or solution treatment) influences subsequent cold working and annealing treatments. This precipitation is irreversible without remelting the alloy.

Munson [14] in a note clarifying the formation of the  $\alpha$ -phase in Al-Fe-Si and Al-Fe-Mn-Si suggested a sequence:

- hexagonal  $\alpha$ -Al-Fe-Si
- bcc  $\alpha$ -Al-Fe-Mn-Si
- simple cubic  $\alpha$ -Al-Mn-Si

noting that the latter phase will take Fe into solid solution. No analysis data was reported for the phase.

Electron diffraction patterns (e.g. Fig. 3) for

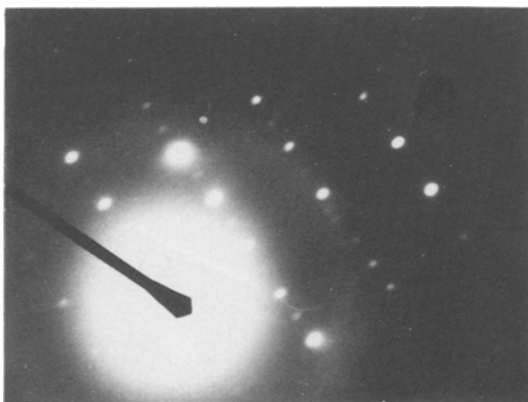


Figure 3 Single-particle electron diffraction pattern from a 0.1  $\mu\text{m}$   $\alpha$ -phase particle showing  $\langle 100 \rangle$  superlattice reflections. Electron beam direction  $[013]$ .

the small particles in the present study show the presence of additional weaker reflections which suggest a simple cubic structure or, perhaps, an ordered form of the bcc phase, as suggested by Furrer and Hausch [14]. There was an insufficient volume of small particles in the suspension to enable the detection of the superlattice lines in the X-ray diffraction traces.

In this paper it has been noted that the large particles, which formed in the interdendritic liquid during solidification, have a higher iron-to-manganese ratio and a lower silicon content than the particles precipitated during high-temperature heat treatment. It is suggested that aluminium can occupy silicon sites in the structure. To the best of our knowledge the stoichiometry of the phase has not been properly established. The crystal structure report [8] on the  $\alpha$ -phase did not distinguish between aluminium and silicon sites. The crystal used for the structure determination had a composition 28.4 wt% Mn, 10.7 wt% Si, 60.9 wt% Al, a composition very close to the composition found in this work for the smaller particles. This composition suggests the formula:  $\text{Al}_{18}\text{Mn}_4\text{Si}_3$  or perhaps  $\text{Al}_{12}\text{Mn}_3\text{Si}_2$  and certainly not  $\text{Al}_{12}\text{Mn}_3\text{Si}$ .

However, the analysis of large particles suggests a formula quite close to  $\text{Al}_{12}\text{Mn}_3\text{Si}$ , or perhaps  $\text{Al}_{13}\text{Mn}_3\text{Si}$ , bearing in mind the crystal structure. This suggests that the form of the  $\alpha$ -phase which forms from the melt has half the silicon atoms replaced by aluminium atoms.

## 5. Conclusions

The extraction of particles from complex aluminium alloys using 8-hydroxyquinoline is a suitable method for obtaining information on the structure and composition of insoluble intermetallic phases in aluminium alloys.

Two forms of the  $\alpha$ -Al-Fe-Mn-Si phase were found in alloy 6010:

(a) Large irregular-shaped particles of approximate formula  $\text{Al}_{13}(\text{Fe Mn})_3\text{Si}$  which formed during solidification, having a body centred cubic structure with lattice parameter 1.260 nm and Mn/Fe ratio of 0.5.

(b) Smaller spheroidal or cylindrical particles formed during high-temperature heat treatment conforming to  $\text{Al}_{12}(\text{Fe Mn})_3\text{Si}_2$  and having an ordered bcc or simple cubic structure. The lattice parameter of this phase was 1.258 nm and the Mn/Fe ratio was 2.4.

The  $\alpha$ -phase absorbs solute elements, particularly copper and silicon, during ageing at 200° C.

## References

1. H. MODIN and S. MODIN, "Metallurgical Microscopy", (Butterworths and Co. London, 1968) p. 288.

2. W. L. MANKIUS, B. E. LEWIS and J. A. MARTIN, in "Metals Handbook", Vol. 8 (American Society for Metals, Metals Park, Ohio, 1973) p. 102.
3. F. HONDA and K. HIROKAWA, *Z. Anal. Chem.* **262** (1972) 170.
4. F. H. COCKS, M. L. SHEPHARD and H. G. CHILTON, *J. Mater. Sci.* **12** (1977) 494.
5. F. COGAN, W. GAYLE, D. KLEIN, F. H. COCKS and M. L. SHEPHARD, *ibid.* **13** (1978) 2687.
6. Patent, Soviet 487339, See World Aluminium Abstracts, 7705-72-0068P (1977).
7. G. W. LORIMER and G. CLIFF, *J. Microscopy* **103** (1975) 203.
8. ASTM Powder Diffraction File 6-0669.
9. M. COOPER and K. ROBINSON, *Acta Cryst.* **20** (1966) 614.
10. L. F. MONDOLFO, "Aluminium Alloys: Structure and Properties" (Butterworths and Co., London, 1976) p. 663.
11. H. WARLIMONT, *Aluminium* **53** (1977) 171.
12. J. I. GOLDSTEIN, in "Introduction to Analytical Electron Microscopy" edited by J. J. Hren, J. I. Goldstein and D. C. Joy (Plenum Publishing Co. New York, 1979).
13. P. L. MORRIS and B. J. DUGGAN, *Metal Science* **12** (1978) 1.
14. D. MUNSON, *J. Inst. Metals* **95** (1967) 217.
15. P. FURRER and G. HAUSCH, *Metal Sci.* **13** (1979) 155.

Received 6 October and accepted 14 November 1980.